Hindawi Publishing Corporation
International Journal of Manufacturing Engineering
Volume 2014, Article ID 596128, 12 pages
http://dx.doi.org/10.1155/2014/596128

Research Article

Enhancing Multistage Deep-Drawing and Ironing Manufacturing Processes of Axisymmetric Components: Analysis and Experimentation

F. Javier Ramírez,[1,2] Rosario Domingo,[3] Michael S. Packianather,[4] and Miguel A. Sebastian[3]

[1] *EXPAL Systems, Avenida Partenón 16, 28042 Madrid, Spain*
[2] *School of Industrial Engineering, University of Castilla-La Mancha, Albacete, Spain*
[3] *School of Industrial Engineering, UNED, 28042 Madrid, Spain*
[4] *School of Engineering, Cardiff University, Cardiff, UK*

Correspondence should be addressed to F. Javier Ramírez; franciscoj.ramirez@uclm.es

Received 7 February 2014; Accepted 4 May 2014; Published 29 May 2014

Academic Editor: Jean-Yves Hascoet

An optimization technique for combined processes of deep-drawing and ironing has been created in order to improve the total process time and cost in manufacturing procedures of axisymmetric components. The initial solution is optimized by means of an algorithm that minimizes the total time of the global process, based on relationship between lengths, diameters, and velocities of each stage of a multistage process and subject to constraints related to the drawing ratio. The enhanced solution offers a significant reduction in time and cost of the global process. The final results, applied to three cases, are compared with experimental results, showing the accuracy of the complete solution.

1. Introduction

The industry of metallic components manufacturing requires developments to be more efficient, in particular in the deep-drawing procedures, where it is important to decrease the process times and costs as in mass production. Thus, it is necessary to devise specific algorithms that will satisfy these demands. These algorithms should be based on technological and scientific basis that will provide solutions that are ready for transfering to the industries. The deep-drawing process has been analysed with this objective in mind due to its convenient nature as a global model which includes all stages of the process, namely, drawing, redrawing, and ironing.

The majority of literature contributions are focused on the study of properties of process, in particular, the prediction of the limiting drawing ratio (LDR) [1–3], the blank design using different methodologies, such as parametric NURBS surfaces [4], upper bound method [5], or artificial neural network [6, 7], the effect of die radius on the blank holder force and drawing ratio [8], the predicted thickness distribution of the deep drawn circular cup of stainless steel [9], the improvement of drawability by means of technological parameters [10, 11] or the formability with different thickness [12]. However, some efforts have been realised about the parts design [13] or generation of algorithms, mainly related to the process planning; Ramana and Rao [14] developed a framework based on knowledge related to design-process planning integration for sheet metal components, although there is no evidence of its application. Also, Vosniakos et al. [15] devised an intelligent system to process design of sheet parts. As can be seen, the researches of deep-drawing processes are not focused on the reduction of time, despite frequently being used on mass production due to the characteristics of the parts.

This paper presents a model that provides a comprehensive analysis of those phenomena occurring in the multistage processes of axisymmetric geometry and applied to the manufacturing of this type of components. The scientific development stems from the work done by Leu [1] and Sonis et al. [2] which provides LDR solutions based on normal

anisotropy value, strain hardening exponent, and others, applied to the drawing and redrawing stages. The model [16, 17] has a scientific foundation based on the literature covering the plastic deformation processes and, in particular, drawing [18], redrawing [19], and ironing. This study focuses on analyzing geometries of axisymmetric components, manufactured by a multistage deep-drawing process.

The drawing processes from a blank [6, 8] have been researched and their governing equations are well known [3, 5]. However, the redrawing and ironing phenomena have received relatively less attention [2, 20]. This work contributes to the definition of a global process of drawing, redrawing, and ironing combined process, together with a common focus on the drawing process in order to obtain a global solution.

The model is used to carry out a quantitative and integrated analysis in a multistage deep-drawing process based on a scientific solution and real measurements. Also, the model permits the modification for some process variables to predict their influence on the process [9]. In addition, it is based on the definition of limiting conditions to guarantee the stability of the process. The simultaneous accomplishment of limiting situations of each process (drawing, redrawing, and ironing) allows for fixing a boundary for the values of each stage which gives the initial solution. The model permits the optimisation of the initial solution from several points of view: total process time, manufacturing cost, among others, such as punch and die wear. This optimisation is based on the resolution of an algorithm by means of recursive functions, which explores all the possibilities of the process and selects the most adequate one. The algorithm is supported by a software tool that provides the optimized solution [21]. The optimized solution is compared with the experimental results.

The remainder of the paper is organised as follows. In Section 2, the methodology used is formulated and applied to some industrial cases. In Section 3, the initial solution found from the scientific model is presented. Section 4 defines the optimization process. In Section 5, the optimization algorithm for solving the multistage process is proposed. In Sections 6 and 7, the simulated and experimental results are compared in order to show the reliability of the complete solution found by the proposed algorithm.

2. Methodology

The methodology used in the definition and resolution of the algorithm is based on a model that departs from an initial solution, defined by the technological constraints that characterize the multistage deep-drawing processes (see Section 3). The use of these processes in mass production will require the minimization of the total process time and the quantity of raw material, thus acting as constraints.

The algorithm resolution has been carried out by the software called deep-drawing tool (DDT) developed by the author. This tool allows the user to perform the total multistage process; it allows the evaluation of the most important variables of the process and the implementation of the optimization algorithm which is the objective of this paper.

Table 1: Brass UNS C26000 properties.

Material	UNS C26000
Density, ρ	8.53 Kg/dm^3
Material rigid-plastic constant, C	895.0 MPa
Strain hardening exponent, n	0.485
Tensile strength, yield, S_y	435.0 MPa
Tensile strength, ultimate, S_u	525.0 MPa
Normal anisotropy value, R	0.83

Table 2: Dimensions of parts (in mm).

	Case A	Case B	Case C
External diameter, d_n	98.5	134.4	102.7
Length, l_n	620	650	1,480
Bottom thickness, s_n	13.5	13.8	15
Wall thickness, e_n	2	1.45	0.95

The algorithm results are contrasted experimentally by means of the resolution of several industrial cases. The applied product type is an axisymmetric component produced in brass by multistage deep-drawing and ironing processes. The use of this material is justified due to its good properties suitable for these multistage processes. Table 1 shows the characteristics of brass UNS C26000 used on the resolution of the industrial cases presented in Section 5.

The solutions provided by this algorithm have been tested against three industrial cases and geometries as shown in Table 2.

The resolution of these types of cases requires the combination of different processes of drawing, redrawing, and ironing. Figure 1 shows the drawing and redrawing/ironing press used on the manufacturing processes of the industrial cases. Figure 2 shows some of the manufacturing stages for Case A.

3. Model Approach

Figure 3 shows the flow diagram of the model providing the initial solution: model phases, input variables required to define the "new project," and the flow information between different stages. The model develops the required solution from the input data. These input data correspond to the dimensions and material of the final piece. The required input data are the external diameter (d_n), the length (l_n), bottom thickness (s_n), wall thickness (e_n), and the material type. The model permits the selection of the material type and its mechanical characteristics needed to form the part: density, ρ (kg/m^3); ultimate tensile strength, S_u (MPa); yield tensile strength, S_y (MPa); material rigid-plastic constant, C (MPa); strain hardening exponent, n; and normal anisotropy value, R. From the input data, the dimensions of the initial part or blank are calculated based on the incompressibility condition of the plastic deformation. This condition considers that the volume of the piece is unchanged throughout the deformation process [18]. A detailed formulation about the previous model that determines the initial solution can be found in

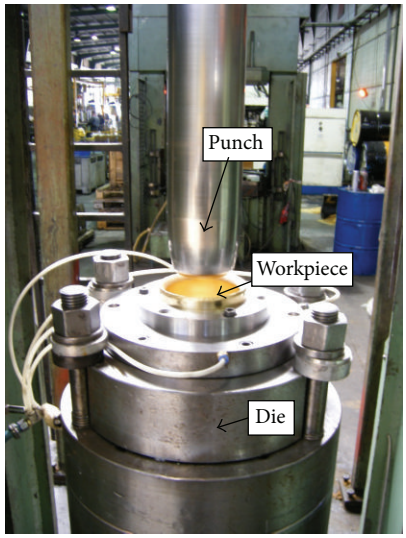

Figure 1: Redrawing and ironing press.

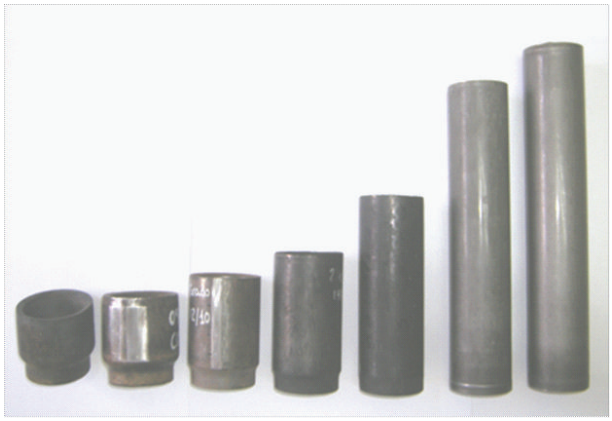

Figure 2: Case A: manufacturing stages.

Ramirez et al. [22]. The dimensions of this blank are the starting point to develop the drawing, redrawing, and ironing processes until the required final dimensions are achieved. In this way, data from the blank becomes the input for the next step: drawing.

3.1. Drawing. The model presents a calculation procedure for each process: drawing, redrawing, and ironing. The determination of the initial solution is treated independently for each of the threads that may occur. It is important to note that, depending on the type of piece, in some cases, its geometry is not necessary to consider redrawing or ironing stages. For determining the initial solution of the drawing, a hypothesis that would later be amended in the adjustment of the technological process is used, and it is the size of the diameter of the punch corresponding to that stage. The LDR is a measure of deep draw ability which defines the largest blank that can be drawn without tearing. It is the ratio between the maximum blank diameter and punch diameter. The design of this punch will depend on the LDR and the final dimensions of the piece. It is also possible that this diameter is changed later in the adjustment of the technological process in order to allow a clearance between the punch and the workpiece for subsequent stages of redrawing and ironing [20]. The solution for the initial stage of drawing is calculated by considering two limiting conditions as described below. The model selects the drawing diameter or the die, d, by using the largest diameter ($d_{1,1}$ and $d_{1,2}$) obtained from the two drawing conditions. Once the diameter is known, the model determines all the dimensions needed to define the drawing stage. Verification of the drawing stage dimension is conducted using two experimental conditions based on empirical studies and collected field data. The corresponding flow diagram is shown in Figure 4.

The first limiting drawing condition is related to the maximum force ($F_{e,\max}$) executed by the punch on the workpiece during the drawing process, which must be less than the cracking load of the material (F_{cr}), according to (1). These forces establish the range in which the force can be obtained using from the efficiency coefficient (η_{def}), ultimate tensile strength, blank thickness (s_0), and the initial (d_0) and final (d_1) diameters (note that the mean wall diameter is $d_{m,1} = d_1 + s_0$), and they are based on the experimental expression from Siebel and Beisswänger [23]. This condition requires the following:

$$F_{e,\max} = \pi \cdot d_{m,1} \cdot s_0 \left[1.1 \cdot \frac{1.3 S_u}{\eta_{\text{def}}} \left(\ln \frac{d_o}{d_1} - 0.25\right)\right],$$
$$F_{\text{cr}} = \pi \cdot d_{m,1} \cdot s_0 \cdot S_u. \quad (1)$$

The second drawing limiting condition is calculated by using the expression developed by Leu [1], which showed good agreement between theoretical and experimental results [2, 3]. Considering the condition of constant volume throughout the process of plastic deformation, LDR can be defined as follows:

$$\text{LDR} = \sqrt{e^{(2fe^{-n\sqrt{(1+R)/2}})} + e^{(2n\sqrt{(1+R)/2})} - 1}. \quad (2)$$

This expression estimates the LDR as a function of normal anisotropy, the strain hardening exponent, and efficiency (f).

In this manner, upper and lower bounds are established, considering the materials proprieties and the drawing capacity. The two limiting conditions use new data from the blank geometry and process efficiency (η_{def} and f).

3.2. Redrawing. Once the dimensions of the drawing stage are obtained, the model provides these data as input values for the next phase of the process: redrawing. The goal of this step is to obtain the final dimensions of the piece needed to perform the next step: ironing. The solution for the initial stage of redrawing is calculated from the consideration of three limiting conditions as described below. The model selects the diameter of the die from the largest of the solutions obtained in the three redrawing constraints ($d_{1\cdot n,1}$, $d_{1\cdot n,2}$, and $d_{1\cdot n,3}$). Once the diameter is known, the model determines all dimensions needed to define this stage. Figure 5 presents the flow diagram of this redrawing algorithm.

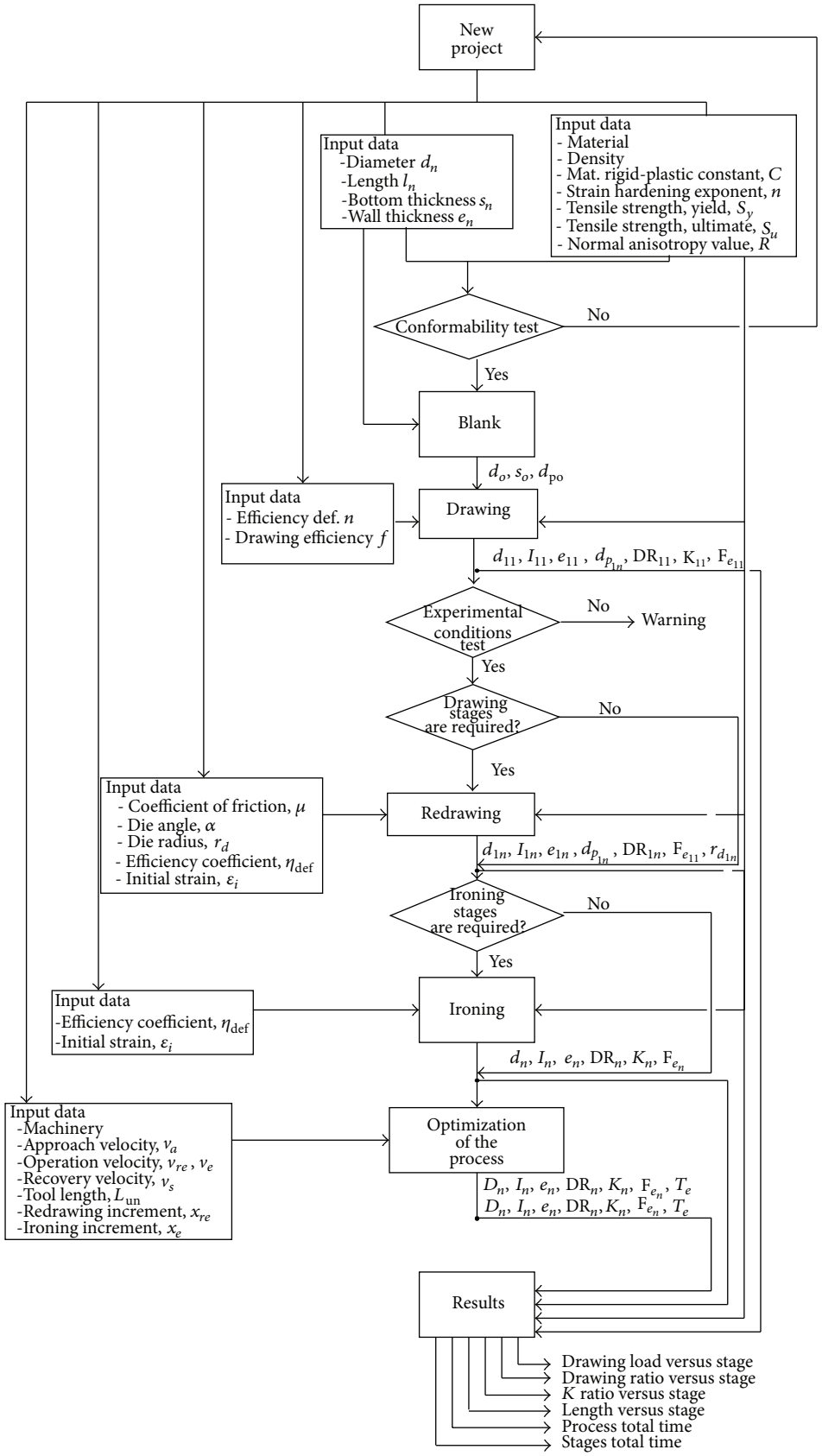

Figure 3: Flow diagram of the model.

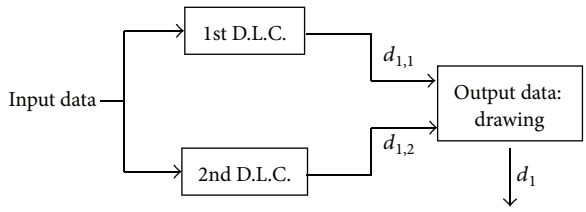

(D.L.C.: drawing limiting condition)

Figure 4: Flow diagram of the drawing algorithm.

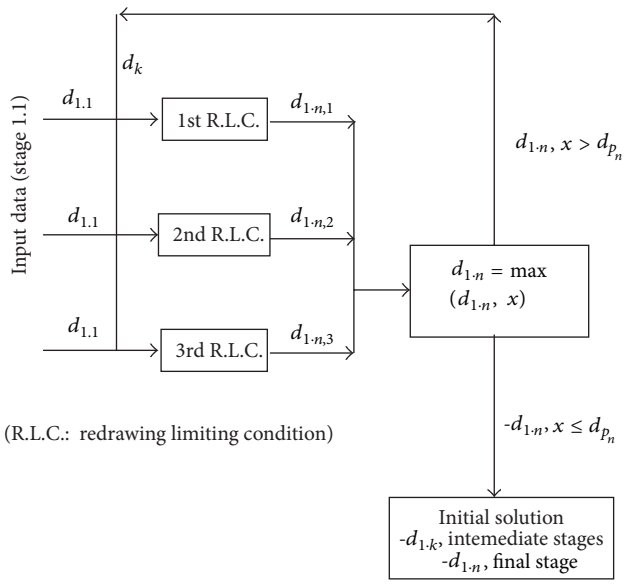

(R.L.C.: redrawing limiting condition)

Figure 5: Flow diagram of the redrawing algorithm.

The first redrawing limiting condition is related to the redrawing load of the punch during the process of redrawing ($F_{\text{re,max}}$), which must be less than the cracking load of the material (F_{cr}), according to (3) and (4), respectively. Consider

$$F_{\text{re,max}} = \pi \cdot d_{m,1\cdot n} \cdot s_{1\cdot n} \cdot 1.3 S_u \left[2e^{\mu\pi/2} \frac{d_{p,1\cdot n} - d_{m,1\cdot n}}{d_{p,1\cdot n} + d_{m,1\cdot n}} 1.1 + \frac{\mu}{\tan\alpha} + \frac{s_{1\cdot n}}{2r_D} \right], \tag{3}$$

$$F_{\text{cr}} = \pi \cdot d_{m,1\cdot n} \cdot s_{1\cdot n} \cdot S_u. \tag{4}$$

The first condition is based on Siebel and Beisswänger [23], where μ is the friction coefficient, α is the die half-angle, d_p is the punch diameter, and r_D is the die radius.

The second redrawing limiting condition assumes the *rigid-plastic condition of the material.* Assuming that the material behaves according to a parabolic law that approximates the potential behaviour of metallic materials cold-manufactured, then it is possible to determine an expression relating the external diameter of the part of a generic step of the process of redrawing, $d_{1\cdot n}$, to the diameter of the previous stage. Assuming the material is annealed ($\varepsilon_i = 0$) and considering the total deformation between the initial and final states, the condition takes the following form:

$$d_{1\cdot n} = d_{1\cdot n-1} e^{-\varepsilon_f/2}. \tag{5}$$

The third redrawing limiting condition is referred to as the *limiting drawing ratio*. In applying the third limiting condition of drawing, the model applies the formulation defined by Sonis et al. [2] about the LDR study in the operations of redrawing. The model considers the effects of the normal anisotropy of the material, friction coefficient, coefficient of strain hardening, and the radius of the input die (r_d). The LDR is used in this model as a variable to determine the required number of redrawing steps and size of the stages. It is assumed that the material is rigid-plastic [2]. Moreover, assuming that the material is rotationally symmetric, the same properties are based on the existence of normal anisotropy and planar isotropy. The Sonis model [2] is based on the tension that is created in the area of the radius of the die redrawing causing instability in the plastic wall of the cup, which is equal to the radial tension in the drawing area of the flange, due to the continuity of tension throughout the piece. Based on the Sonis model, the expression for LDR_i can be written as

$$\begin{aligned} f(\text{LDR}_i) &= -\frac{C_1 \cdot r_{c_{(i-1)}}}{r_{c_{(i-1)}} + \text{LDR}_{(i-1)} \cdot r_d} + \frac{C_3 \cdot r_{c_{(i-1)}}}{r_d + r_{c_{(i-1)}}/\text{LDR}_{(i-1)}} \\ &\quad + C_4 \ln\left(\frac{r_{c_{(i-1)}}}{r_d + r_{c_{(i-1)}}/\text{LDR}_{(i-1)}} \right) \\ &\quad + C_5 \ln\left(\frac{r_{c_{(i-1)}}}{r_d + r_{c_{(i-1)}}/\text{LDR}_{(i-1)}} \right) \\ &\quad - \frac{1}{\left(r_d + r_{c_{(i-1)}}/\text{LDR}_{(i-1)}\right)^2 \left(\left(R_{(i+1)}/r_{cd}\right)^2 - 1\right)} \\ &\quad \times \left[r_{c_{(i-1)}} \right. \\ &\quad \times \sqrt{\left(r_d + \frac{r_{c_{(i-1)}}}{\text{LDR}_{(i-1)}}\right)^2 \left(\left(\frac{R_{(i+1)}}{r_{cd}}\right)^2 - 1\right) + r_{c_{(i-1)}}^2} \\ &\quad - \left(r_d + \frac{r_{c_{(i-1)}}}{\text{LDR}_i}\right)^2 \left(\frac{R_{(i+1)}}{r_{cd}}\right) \\ &\quad \left. - \left(r_{c_{(i-1)}}^2 - \left(r_d + \frac{r_{c_{(i-1)}}}{\text{LDR}_i}\right)\right)^2 \right] \\ &\quad + C_5 \ln\left[r_{c_{(i-1)}} \right. \\ &\quad \left. + \sqrt{\left(r_d + \frac{r_{c_{(i-1)}}}{\text{LDR}_{(i-1)}}\right)^2 \left(\left(\frac{R_{(i+1)}}{r_{cd}}\right)^2 - 1\right) + r_{c_{(i-1)}}^2} \right] \\ &\quad - C_5 \ln\left(\left(\frac{r_d + r_{c(i-1)}}{\text{LDR}_i}\right) \left(1 + \frac{R_{(i+1)}}{r_{cd}}\right) \right) = 0, \end{aligned} \tag{6}$$

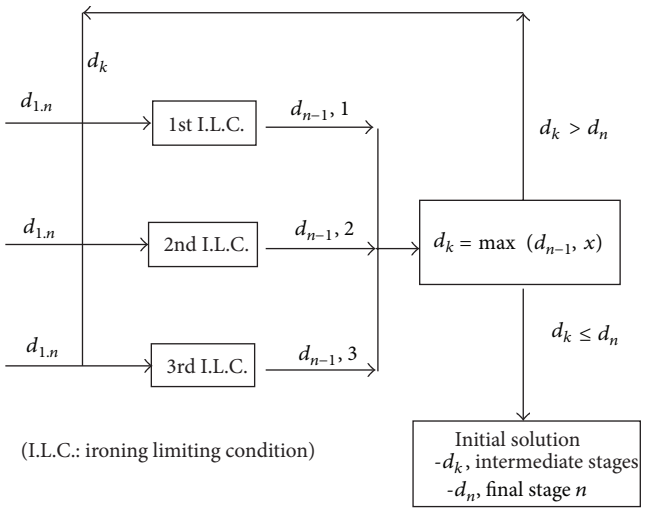

Figure 6: Flow diagram of the ironing algorithm.

where C_1, C_3, C_4, and C_5 are constants, r_c is the corner radius, and r_{cd} is the die opening radius [2].

Based on the previous expressions in the function under the LDR, an expression depending on the LDR is obtained, and the nonlinear equations are solved by the Newton-Raphson method. In this way, it is possible to determine the values of LDR for each stage of redrawing, starting from an initial die radius and by the consideration that the die radius of each redrawing step will be reduced until 80% of the corresponding value of the previous phase. Once the LDR for each redrawing phase is found, the model determines the diameter of each stage.

3.3. Ironing. The number of stages of ironing depends on the size of the final part. The model is based on the performance of three limiting conditions to be drawn from stage 2 to stage n. The calculation of the process variable is the external diameter of the piece, according to the block diagram, illustrated in Figure 6.

By considering separately the merits of the three limiting conditions for ironing, the solution can be determined for phases 2 to n.

The First Ironing Limiting Condition. The maximum ironing load ($\sigma_{e,\max}$) must be less than the cracking load (σ_r) of the material. This condition is expressed as the following:

$$F_{e,n-1} < \frac{\pi}{4} \cdot \left(d_{n-2}^2 - d_{n-1}^2\right) \cdot n \cdot S_u. \tag{7}$$

Second Ironing Limiting Condition. This condition assumes that the maximum load in the ironing process (σ_e) must be less than the yield tensile strength ($Y(\varepsilon_f)$). This condition provides good results in parts of drawing [24] and it requires

$$\frac{C}{n+1}\left({\varepsilon_f}^{n+1} - {\varepsilon_i}^{n+1}\right) < Y\left(\varepsilon_f\right) \equiv C \cdot {\varepsilon_f}^n. \tag{8}$$

Third Ironing Limiting Condition. This refers to the value of the thickness reduction ratio limit (K). This ratio is widely used in the calculation and design of the processes of drawing [5]. The model performs the calculation for each K stage, which mainly depends on the stage of drawing and the type of material used.

4. Optimization Process

The model is based on the minimization of the total process time, which is the time to approach the punch from the initial stage, plus the time of the operation, plus the time to recover the punch to its initial position, according to the following objective function:

$$F_o = \min t_e = \min \sum_{i=1}^{n} t_i = \min \sum_{i=1}^{n} \left(t_{a,i} + t_{o,i} + t_{s,i}\right), \tag{9}$$

where F_o is the objective function, t_e is the total process time, t_i is the total process time at stage i, $t_{a,i}$ is the approach time at stage i, $t_{o,i}$ is the operation time at stage i, and $t_{s,i}$ is the recovery time at stage i.

The process time at stage i is given by the expression

$$t_i = \frac{1.1 \cdot l_{i-1}}{v_{a,i}} + \frac{L_{ui} + l_i}{v_{e,i}} + \frac{1.1 \cdot l_{i-1} + L_{ui} + l_i}{v_{s,i}}, \tag{10}$$

where l_{i-1} is the part length in stage $i-1$, L_{ui} is the punch length in stage i, l_i is part length in stage i, $v_{a,i}$ is the approach velocity of the press in the stage i, $v_{e,i}$ is the ironing velocity in the stage i, and $v_{s,i}$ is the recovery velocity of the press in the stage i.

As can be seen, the time is defined by means of the velocities involved in each operation and the punch or part length of each stage. Moreover, the part length in stage i is related to the bottom thickness, the blank diameter, the punch diameter, and the optimized diameter. Therefore, the model presents an optimization problem with an objective function which is subject to some constraints as follows:

$$\begin{aligned} F_o &= \min t_e = \min \sum_{i=1}^{n} t_i \\ &= \min \sum_{i=1}^{n} \left(\frac{1.1 \cdot l_{i-1}}{v_{a,i}} + \frac{L_{ui} + l_i}{v_{e,i}} + \frac{1.1 \cdot l_{i-1} + L_{ui} + l_i}{v_{s,i}} \right) \end{aligned} \tag{11}$$

subject to

$$d_n \leq D_n \leq d_n\left(1 + \Delta DR_e\right), \tag{12}$$

where

$$l_i = \frac{s_i\left(d_o^2 - d_{p,i}^2\right)}{\left(D_i^2 - d_{p,i}^2\right)}, \tag{13}$$

and D_i is the optimized diameter in stage i, s_i is the bottom thickness in stage i, $d_{p,i}$ is the punch diameter in stage i, and ΔDR_e is the drawing surplus ratio between the stages n and m, defined by the expression

$$\Delta DR_e = DR_m - DR_n. \tag{14}$$

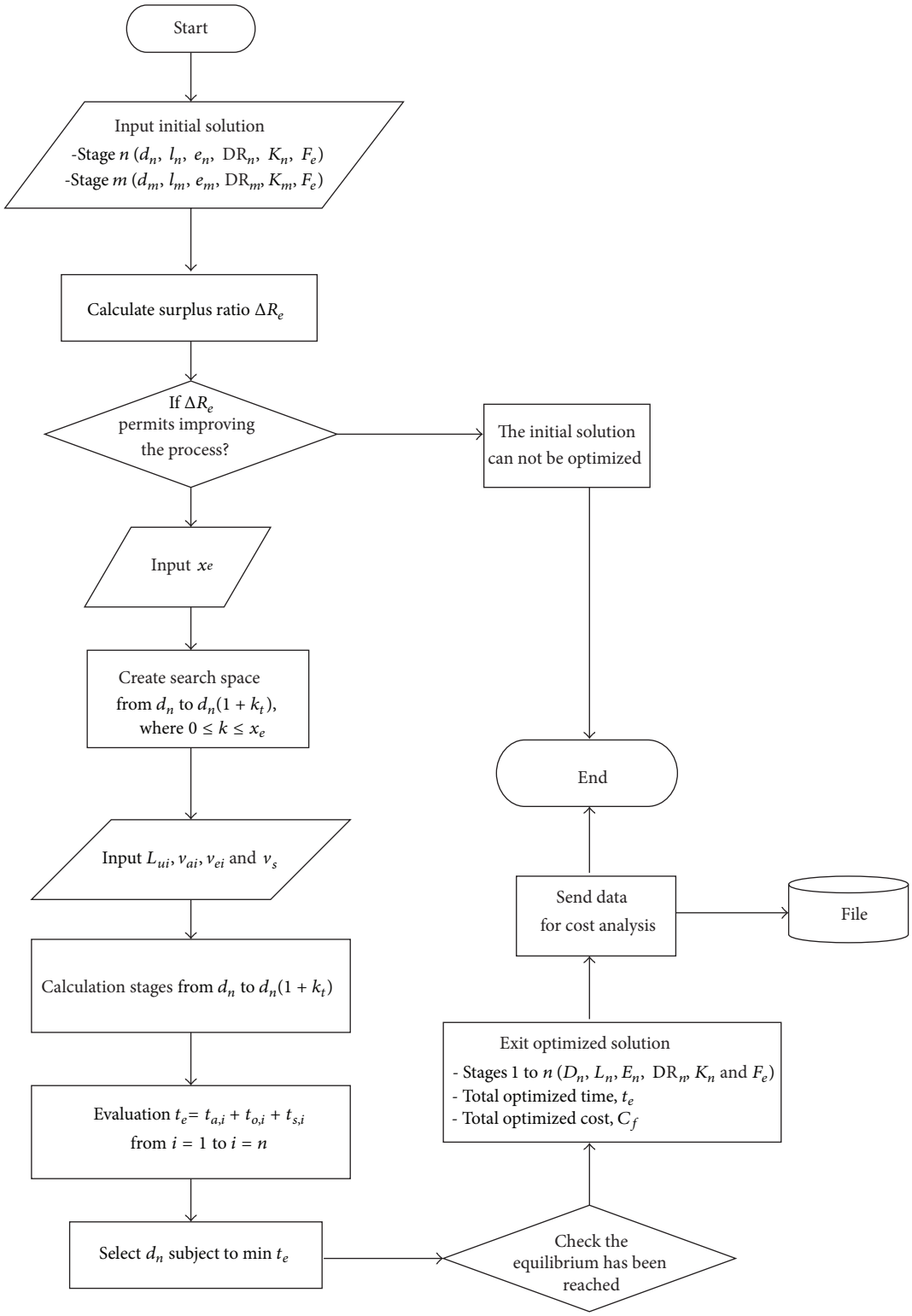

Figure 7: Flowchart of the algorithm.

The optimization requires a distribution between the stages 1 to n of the drawing surplus ratio, ΔDR_e. This distribution is conditioned to the minimization of the total process time as the sum of each stage time. Thus, an improvement is achieved in each drawing stage. In this manner, the optimized drawing conditions are separate from the maximum limits fixed by the initial drawing conditions.

The resolution of the recursive function is carried out according to the values of all the possible diameters between d_n and $d_n(1 + \Delta DR_e)$. The algorithm identifies which combination is the most suitable, and it selects the optimized diameter D_n in each stage, such that the condition of the objective function is satisfied; that is, the combination of diameters must give the minimum total process time.

The algorithm also permits the modification of the velocity parameters in each press required in the multistage process (approach velocity, operation velocity, and recovery velocity of the punch). Accordingly, it is possible to realise a more adequate distribution of available presses in the facility.

5. Algorithm Resolution Process

The algorithm proposed in Figure 7 performs the resolution in the following steps.

Step 1. Definition of incremental factor t, given by the following expression:

$$t = \frac{\Delta DR_e}{x_e}, \tag{15}$$

where ΔDR_e is the surplus ratio of drawing and x_e is the number of times that the drawing surplus ratios are fractioned.

Step 2. Progressive increment of diameter of each process stage, from d_n to $d_n(1 + kt)$, where k is a parameter that varies from 0 to factor x_e.

Step 3. Resolution of the recursive function is based on obtaining all possible substages, by means of the modification of each stage diameters, from d_n to $d_n(1 + \Delta DR_e)$.

Step 4. Once all the possible diameters of each stage are defined, the algorithm searches the arrangement that allows for the minimizing of the total process time.

Step 5. The search stops and the best solution up to the current iteration is given as the output.

6. Experimental Results

The deep-drawing tool has allowed for the verification of this algorithm's integrity. Computational and experimental tests have been carried out in brass, in particular in UNS C26000 alloy, applied to three parts. The dimensions of the parts are shown in Table 2.

For the experimental results of the three cases presented in Table 2, its analytical resolution has been carried out by the software DDT according to the flowchart presented in Figure 3. The final result of using the software tool is an improved solution that optimizes the total process time and reduces the manufacturing cost of the presented industrial cases. These costs use the information from the results provided by the previous steps and are based on the total time of the deformation process and the labour cost per hour.

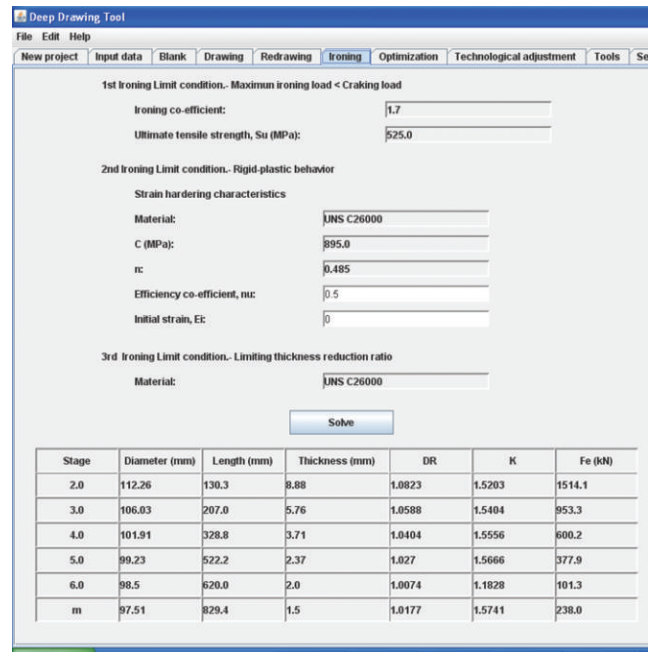

Figure 8: Case A: initial solution results.

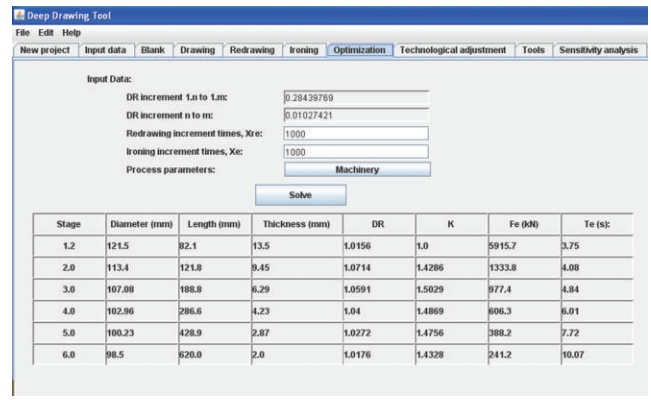

Figure 9: Case A: optimization process results.

Figure 8 shows the results of the tool for the initial solution corresponding to Case A.

Figure 9 presents the calculation of the optimized process by means of the DDT using the proposed algorithm. Values for x_{re} and x_e in operations of redrawing and ironing are given.

The resolution of the optimization process using the proposed algorithm requires the introduction of the machinery operation parameters involved in the process.

The computer tool requires the input of these data (Figure 10), according to the flowchart of the algorithm presented in Figure 3.

One of the most important variables in the analysis of such processes is the variable "ratio of wall thickness reduction." The optimization process allows the user to obtain a greater stability of the process maintaining the balance of the different phases. Table 3 shows the evolution of the drawing load for the industrial Cases A, B, and C under study.

Table 3: Evolution of drawing load.

Stages	Case A		Case B		Case C	
	Initial solution (IS)	DDT algorithm solution	Initial solution (IS)	DDT algorithm solution	Initial solution (IS)	DDT algorithm solution
Drawing						
Stage 1.1	3188.5	3188.5	3175.0	3175.0	3692.1	3692.1
Redrawing						
Stage 1.2	5915.7	5915.7	—	—	—	—
Ironing						
Stage 2.0	1514.1	1346.4	2082.3	1859.8	1803.8	1710.1
Stage 3.0	953.3	962.6	1311.1	1320.5	1135.7	1141.1
Stage 4.0	600.2	626.8	825.5	859.3	715.1	718.6
Stage 5.0	377.9	381.4	519.8	523.2	450.2	452.6
Stage 6.0	101.3	229.8	327.3	329.5	283.5	285.0
Stage 7.0			15.8	189.3	178.5	179.4
Stage 8.0					32.4	112.4

Table 4: Evolution of wall thickness.

Stages	Case A		Case B		Case C	
	Initial solution (IS)	DDT algorithm solution	Initial solution (IS)	DDT algorithm solution	Initial solution (IS)	DDT algorithm solution
Drawing						
Stage 1.1	1	1	1	1	1	1
Redrawing						
Stage 1.2	1	1	—	—	—	—
Ironing						
Stage 2.0	1.520	1.434	1.535	1.450	1.518	1.477
Stage 3.0	1.540	1.494	1.552	1.505	1.538	1.516
Stage 4.0	1.555	1.511	1.564	1.519	1.554	1.520
Stage 5.0	1.566	1.474	1.572	1.479	1.565	1.512
Stage 6.0	1.182	1.412	1.578	1.442	1.573	1.492
Stage 7.0			1.028	1.345	1.578	1.459
Stage 8.0					1.11	1.409

Table 4 shows the evolution of the wall thickness. The results show that the optimized process achieves a better balance so that it is more stable. This stability is transmitted in a better distribution of the capabilities of drawing, redrawing, and ironing between the different stages, subsequently resulting in improved processing time and reduced manufacturing cost.

Once the evolution of different variables that influence the process has been analyzed, the results for "process time" and "manufacturing cost" are presented in order to study the improvements that could be achieved by the implementation of the proposed algorithm.

Tables 5 and 6 show the evolution of these improvements on the variables "total process time" (t_e) and "manufacturing cost" (C_m) in terms of number of iterations performed by the algorithm.

Similarly, the evolution of "total process time" and the "manufacturing cost" for Cases B and C has been analyzed. Figures 11 and 12 show the improvements evolution obtained for the three Cases A, B, and C. It can be observed that the greater improvements are achieved in the first iterations (first five according to Case A), but the results improve further as the iteration increases.

7. Analysis and Discussion of the Results

The resolution of the industrial Cases A, B, and C by means of the DDT Algorithm presents important advantages. As shown in Tables 7, 8, and 9, the DDT algorithm produces improvements between 5.17% and 8.18% compared with the initial solution for the process time variable and between 4.40% and 7.78% for the manufacturing cost. In the same manner, the experimental results obtained an improvement between 6.55% and 9.34% for the process time and from 6.60% to 11.55% for the manufacturing cost. These improvements are more relevant in mass production. The most

Table 5: Process time evolution as a function of the algorithm iteration number.

x_e	5	25	50	100	250	500	1000
$t_{e,1}$	42.054	42.054	42.054	42.054	42.054	42.054	42.054
$t_{e,n}$	40.634	40.109	39.998	39.952	39.889	39.813	39.797
% reduction	3.67%	5.02%	5.31%	5.43%	5.59%	5.79%	5.83%

Table 6: Manufacturing cost evolution as a function of the algorithm iteration number.

x_e	5	25	50	100	250	500	1000
Cm_1	34.974	34.974	34.974	34.974	34.974	34.974	34.974
Cm_n	33.554	33.029	32.918	32.872	32.809	32.733	32.717
% reduction	4.06%	5.56%	5.88%	6.01%	6.19%	6.41%	6.45%

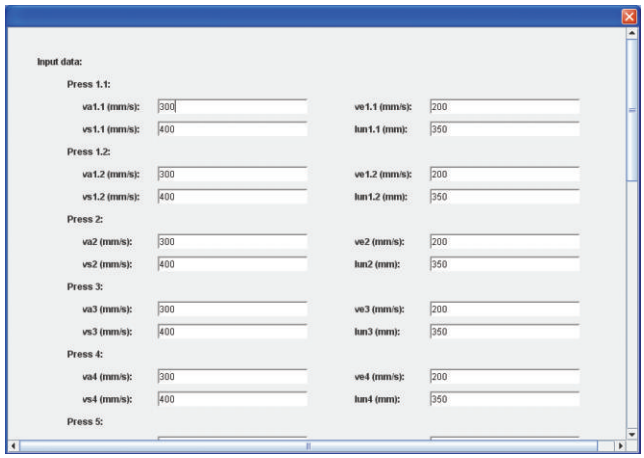

Figure 10: Machinery parameters.

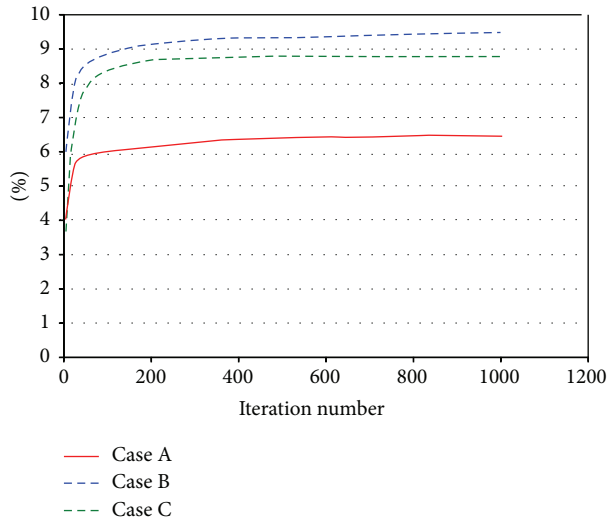

Figure 11: Cases A, B, and C: process time improvements as function of the algorithm iteration number.

significant advances have been achieved in Case B, which represent the highest progress according to the algorithm iteration number (see Figures 11 and 12). Also there is similarity between this algorithm iteration number and Cases A and C where the trend is the same in all cases. The final

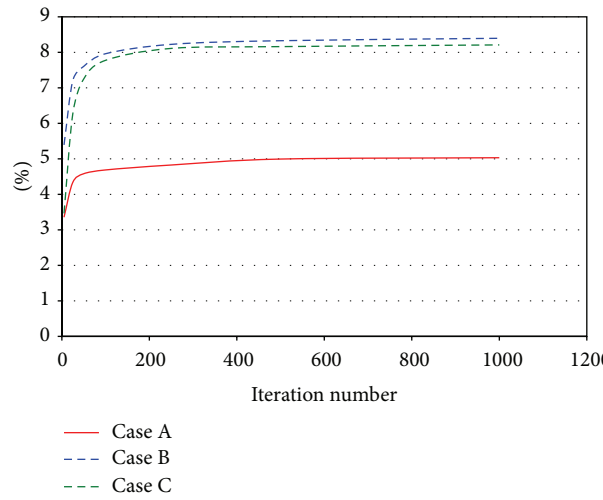

Figure 12: Cases A, B, and C: manufacturing cost improvements as function of the algorithm iteration number.

Table 7: Case A: analysis of the results.

Comparative analysis	Process time	Manufacturing cost per unit
Initial solution (IS)	34.83 s	0.318€
DDT algorithm solution	33.03 s	0.304€
Experimental solution (EXS)	32.55 s	0.297€
DDT versus IS improvement	5.17%	4.40%
EXS versus IS improvement	6.55%	6.60%
EXS versus DDT accuracy	98.55%	97.7%

geometry of the part does not seem to have a particular effect on the results. This is due to a good definition of initial solution that allows processing the blank.

Comparing the algorithm results with the experimental results shows that the accuracy of the process is very high, obtaining values from 98.41% to 98.74% for the process time variable and from 95.92% to 98.13% for the manufacturing cost. Although there are some disparities between the cases analyzed, these differences are not significant because the accuracy is always above 95% and normally very close to 99%. Thus, the mathematical minimization of the total process

Table 8: Case B: analysis of the results.

Comparative analysis	Process time	Manufacturing cost per unit
Initial solution (IS)	42.4 s	0.398€
DDT algorithm solution	38.93 s	0.367€
Experimental solution (EXS)	38.44 s	0.352€
DDT versus IS improvement	8.18%	7.78%
EXS versus IS improvement	9.34%	11.55%
EXS versus DDT accuracy	98.74%	95.92%

Table 9: Case C: analysis of the results.

Comparative analysis	Process time	Manufacturing cost per unit
Initial solution (IS)	76.58 s	0.688€
DDT algorithm solution	70.95 s	0.639€
Experimental solution (EXS)	69.82 s	0.627€
DDT versus IS improvement	7.35%	7.12%
EXS versus IS improvement	8.83%	8.88%
EXS versus DDT accuracy	98.41%	98.13%

time through the technological variables provides a solution which is very close to the experimental outcomes.

8. Conclusions

In this paper, an algorithm that allows the reduction of the total process times and cost in the manufacturing of axisymmetric components has been presented. The algorithm is based on the minimization of total process time, defined by means of the part dimensions and process velocities, and costs by considering the reduction of material usage, through constraints related to drawing surplus ratio. The algorithm has been enhanced with the use of technological parameters. The simulation results of the algorithm achieved a good agreement with the experimental results obtained for the three cases and caused significant improvements in manufacturing times and costs in the deep-drawing process of axisymmetric parts. The comparison of analytical results obtained with the experimental results has demonstrated the high accuracy of the algorithm, which is of interest for real industrial applications.

Future works will aim to get a more efficient process, from a perspective of sustainable energy, thus achieving an integral solution, in terms of scientific and technological basis.

Conflict of Interests

The authors declare that there is no conflict of interests regarding the publication of this paper.

Acknowledgments

The authors gratefully acknowledge the company EXPAL Systems, S.A., as well as its factory in Navalmoral de la Mata (Cáceres, Spain) for supporting the experimental results presented in this paper.

References

[1] D. K. Leu, "The limiting drawing ratio for plastic instability of the cup-drawing process," *Journal of Materials Processing Technology*, vol. 86, no. 1–3, pp. 168–176, 1998.

[2] P. Sonis, N. V. Reddy, and G. K. Lal, "On multistage deep drawing of axisymmetric components," *Journal of Manufacturing Science and Engineering*, vol. 125, no. 2, pp. 352–362, 2003.

[3] R. K. Verma and S. Chandra, "An improved model for predicting limiting drawing ratio," *Journal of Materials Processing Technology*, vol. 172, no. 2, pp. 218–224, 2006.

[4] R. Padmanabhan, M. C. Oliveira, A. J. Baptista, J. L. Alves, and L. F. Menezes, "Blank design for deep drawn parts using parametric NURBS surfaces," *Journal of Materials Processing Technology*, vol. 209, no. 5, pp. 2402–2411, 2009.

[5] A. Agrawal, N. V. Reddy, and P. M. Dixit, "Determination of optimum process parameters for wrinkle free products in deep drawing process," *Journal of Materials Processing Technology*, vol. 191, no. 1–3, pp. 51–54, 2007.

[6] M. Haddadzadeh, M. R. Razfar, and M. R. M. Mamaghani, "Novel approach to initial blank design in deep drawing using artificial neural network," *Proceedings of the Institution of Mechanical Engineers B: Journal of Engineering Manufacture*, vol. 223, no. 10, pp. 1323–1330, 2009.

[7] A. Chamekh, S. Ben Rhaiem, H. Khaterchi, H. Bel Hadj Salah, and R. Hambli, "An optimization strategy based on a metamodel applied for the prediction of the initial blank shape in a deep drawing process," *International Journal of Advanced Manufacturing Technology*, vol. 50, no. 1–4, pp. 93–100, 2010.

[8] S. Sezek, V. Savas, and B. Aksakal, "Effect of die radius on blank holder force and drawing ratio: A model and experimental investigation," *Materials and Manufacturing Processes*, vol. 25, no. 7, pp. 557–564, 2010.

[9] R. Padmanabhan, M. C. Oliveira, J. L. Alves, and L. F. Menezes, "Influence of process parameters on the deep drawing of stainless steel," *Finite Elements in Analysis and Design*, vol. 43, no. 14, pp. 1062–1067, 2007.

[10] K. Mori and H. Tsuji, "Cold deep drawing of commercial magnesium alloy sheets," *CIRP Annals-Manufacturing Technology*, vol. 56, no. 1, pp. 285–288, 2007.

[11] L. M. A. Hezam, M. A. Hassan, I. M. Hassab-Allah, and M. G. El-Sebaie, "Development of a new process for producing deep square cups through conical dies," *International Journal of Machine Tools and Manufacture*, vol. 49, no. 10, pp. 773–780, 2009.

[12] H. C. Tseng, C. Hung, and C. C. Huang, "An analysis of the formability of aluminum/copper clad metals with different thicknesses by the finite element method and experiment," *International Journal of Advanced Manufacturing Technology*, vol. 49, no. 9–12, pp. 1029–1036, 2010.

[13] B. C. Hwang, S. M. Han, W. B. Bae, and C. Kim, "Development of an automated progressive design system with multiple processes (piercing, bending, and deep drawing) for manufacturing products," *International Journal of Advanced Manufacturing Technology*, vol. 43, no. 7-8, pp. 644–653, 2009.

[14] K. V. Ramana and P. V. M. Rao, "Data and knowledge modeling for design-process planning integration of sheet metal components," *Journal of Intelligent Manufacturing*, vol. 15, no. 5, pp. 607–623, 2004.

[15] G. C. Vosniakos, I. Segredou, and T. Giannakakis, "Logic programming for process planning in the domain of sheet metal forming with progressive dies," *Journal of Intelligent Manufacturing*, vol. 16, no. 4-5, pp. 479–497, 2005.

[16] F. Javier Ramírez and R. Domingo, "Application of an aided system to multi-step deep drawing process in the brass pieces manufacturing," in *Proceedings of the 3rd Manufacturing Engineering Society International Conference, MESIC 2009*, pp. 370–379, Alcoy, Spain, June 2009.

[17] F. J. Ramirez, R. Domingo, and M. A. Sebastian, "Design of an aided system to optimise times and costs in deep drawing process," in *Proceedings of the 2nd IPROMS International Researchers Symposium*, vol. 1, pp. 191–196, Ischia, Italy, 2009.

[18] K. Lange, *Handbook of Metal Forming*, McGraw-Hill, New York, NY, USA, 1985.

[19] S. Y. Chung and S. H. Swift, "An experimental investigation into the re-drawing of cylindrical shells," *Proceedings of the Institution of Mechanical Engineers B: Journal of Engineering Manufacture*, vol. 1, pp. 437–447, 1975.

[20] M. A. Sebastián and A. M. Sanchez-Perez, " Diseño asistido por ordenador de los útiles para la embutición profunda de piezas cilíndricas huecas," Internal Report, ETSII, UPM, Madrid, Spain, 1980.

[21] F. J. Ramirez, R. Domingo, M. A. Sebastian, and M. S. Packianather, "The development of competencies in manufacturing engineering by means of a deep-drawing tool," *Journal of Intelligent Manufacturing*, vol. 24, no. 3, pp. 457–472, 2011.

[22] F. J. Ramirez, R. Domingo, and M. A. Sebastian, "A technological model applied to multi-stage deep drawing process of axisymmetric components," in *Proceedings of the 21st International Computer-Aided Production Engineering Conference (CAPE '10)*, Edinburgh, UK, 2010.

[23] E. Siebel and H. Beisswänger, *Deep Drawing*, Carl Hanser, Munich, Germany, 1995.

[24] E. M. Rubio, M. Marín, R. Domingo, and M. A. Sebastián, "Analysis of plate drawing processes by the upper bound method using theoretical work-hardening materials," *International Journal of Advanced Manufacturing Technology*, vol. 40, no. 3-4, pp. 261–269, 2009.